

*International Symposium*

*on*

MOLECULAR STRUCTURE

*and*

SPECTROSCOPY

PREPRINTS **C**

TOKYO

SEPTEMBER 10-15, 1962

SCIENCE COUNCIL OF JAPAN

Tuesday, September 11      Morning

10 Techniques and Applications      9:00 a.m. - 10:30 a.m.

Chairman      V. J. Coates  
Co-chairman      S. Minami

- C101 (Invited) G. B. B. M. Sutherland  
Interference Spectroscopy and Some of its Applications  
in the Far Infrared and in the Near Infrared
- C102 S. Fujita, H. Yoshinaga, S. Minami, Y. Suemoto, K. Nakano  
and S. Yoshida  
An Idea for a Far Infrared Automatic-Recording Interfero-  
metric Spectrometer and Its Some Experimental Results
- C103 M. E. Vance, R. F. Rowntree, E. E. Bell and R. A. Oetjen  
An Interferometric-Modulation Order-Separator for a  
Far Infrared Spectrometer
- C104 H. Yoshinaga, S. Minami, A. Mitsuishi, I. Makino, K.  
Nakamura, I. Iwahashi, M. Inaba and K. Matsumoto  
An Optical Null Double Beam Far Infrared Spectrometer

10 Techniques and Applications      11:00 a.m. - 12:30 p.m.

Chairman      B. D. Saksena  
Co-chairman      S. Saeki

- C106 (Invited) L. Genzel  
Far Infrared Experimental Techniques
- C107 D. W. Barnes, S. Maeda, G. Thyagarajan and P. N. Schatz  
The Infrared Reflection Spectra of Strong Bands in Liquids
- C108 K. N. Rao  
Infrared Techniques Recently Explored at the Ohio State  
University
- C109 S. Minami, R. A. Oetjen and S. M. Lee  
Optical Null Double-Beam Double-Pass Spectrometer
- C110 H. Makabe, Y. Fukuda, S. Hashizume and M. Kiri  
A High Resolution Infrared Spectrophotometer with a  
Prism-Grating Turntable

Interference Spectroscopy and Some of its  
Applications in the Far Infrared and in the  
Near Infrared

G. B. B. M. Sutherland

National Physical Laboratory, Teddington, Middlesex

About ten years ago Fellgett pointed out the possibility of using a Michelson interferometer to obtain infra-red spectra. The Michelson interferometer produces an interferogram which is the Fourier transform of the spectrum. Conversion from the interferogram to the conventional spectrum is accomplished in a few minutes by a computer. "Spectrometers" based on this idea have special advantages when the resolving power of the conventional spectrometer is limited by the brightness of the source rather than the sensitivity of the detector. At the National Physical Laboratory instruments of this type have been developed by Gebbie for the far infrared region, between  $10\text{ cm}^{-1}$  and  $500\text{ cm}^{-1}$ , and also for the near infrared, between  $10,000\text{ cm}^{-1}$  and  $1000\text{ cm}^{-1}$ . In the former case, the greatest advantage is the speed with which a spectrum can be obtained, e.g. the range from  $20\text{ cm}^{-1}$  to  $500\text{ cm}^{-1}$  can be covered in about 1 hour. In the near infrared, the principal advantage is in the study of emission spectra from sources at moderate temperatures.

The application of these interferometric techniques to a variety of problems will be discussed. In the far infrared, results will be shown for methyl alcohol (hindered rotation of the OH group), hydrogen halides (lattice vibrations in the solid state and pressure/

C 101-2

pressure shifts in the vapour state due to foreign gases), nitrogen (pressure induced absorption) and some organic molecules. In the near infrared, results will be shown for ammonia (emission spectrum at 70°C), luminescent spectra of laser materials and planetary spectra.

# An Idea for a Far Infrared Automatic-Recording Interferometric Spectrometer and Its Some Experimental Results

Shigeru Fujita, Hiroshi Yoshinaga, Shigeo Minami, Yoshiro Suemoto

Department of Applied Physics, Osaka University, Osaka, Japan,

Kaoru Nakano, and Shigeru Yoshida

Central Research Laboratory, Tokyo Shibaura Electric Co., Ltd.,  
Kawasaki, Japan.

The interferometric spectrometer is designed as an instrument which will record automatically the spectrogram in the wavelength region beyond 100 microns translated from the interferogram by a special computer connected to the interferometer.

The interferometer is of Michelson type.<sup>1)</sup> The radiation source is a high-pressure mercury lamp. The beam splitter is made from a film of polyethylene coated with a mixture of germanium and copper by evaporation. The detector is a Golay cell. The sliding table for the movable mirror is carried on balls which roll in the slot between two cylindrical bars.<sup>2)</sup> The displacement of the table is measured by a moiré fringe system<sup>3)</sup> which gives pulses to the computer.

The computer is connected to the interferometer as shown in Fig.1. The output of the detector in the interferometer is fed to the computer after amplification by the ordinary method. Translation of the interferogram to the spectrogram is basically made in the following way.

The relation between the spectrogram  $E(\nu)$  and the interferogram  $F(x)$  is approximated by:

$$\begin{aligned} E(\nu) &= \int_0^{x_m} F(x) A(x) \cos(2\pi\nu x) dx \\ &= \int_0^{x_m} F^*(x) \cos(2\pi\nu x) dx, \end{aligned} \quad (1)$$

where  $x$  is the optical path difference of the two beams,  $x_m$  the maximum value of  $x$ ,  $\nu$  the wave number, and  $A(x)$  an apodization function.

First, the new function  $F^*(x) = F(x)A(x)$  is obtained by the analog computing unit. Then, it is converted to 12 binary digits, including a sign and a space bit, by the A-D converter. The conversion is made by the ordinary method for every step of  $x$ , i.e. at the moment  $x = x_i, i = 1, 2, \dots, m$ .

Integration of Eq.(1) is approximated by the following summation:

$$E(\nu_j) = \sum_{i=1}^m F^*(x_i) \cos(2\pi \nu_j x_i) \Delta x, \quad (2)$$

where  $j = 1, 2, \dots, n$ .

It is assumed that  $\nu_j$ 's are equally spaced and  $\Delta \nu = \nu_n/n$ , where  $\nu_n$  is the maximum value of  $\nu_j$ . The summation of Eq. (2) is performed as follows:

Suppose  $n$  values of  $E_k$  for all  $\nu_j$  i.e.

$$E_k(\nu_j) = \sum_{i=1}^k F^*(x_i) \cos(2\pi \nu_j x_i) \Delta x, \quad (3)$$

are already obtained and stored in a magnetic core memory before the moment when  $x$  is  $x_{k+1}$ . Then,  $E_{k+1}(\nu_j)$  can be calculated by the equation:

$$\begin{aligned} E_{k+1}(\nu_j) &= E_k(\nu_j) + F^*(x_{k+1}) \cos(2\pi \nu_j x_{k+1}) \Delta x \\ &= E_k(\nu_j) + \Delta E_{k+1}(\nu_j) \end{aligned} \quad (4)$$

The calculation is made by the digital computing unit shown in Fig. 2. Each of the stored values of  $E_k(\nu_j)$  is first read out of the memory and the value of  $F^*(x_{k+1}) \cos(2\pi \nu_j x_{k+1}) \Delta x$  is added to it at the accumulator. The value of  $E_{k+1}(\nu_j)$ , thus obtained, is stored back into the memory. This is done in a time of less than a few milliseconds for a single value of  $E_{k+1}(\nu_j)$ . It is possible, therefore, to make these calculations for all of a thousand values of  $\nu_j$ 's in less than a few seconds. The process starts from  $k=1$ , and proceeds to  $k=m$ , or it can be stopped in the course of calculation if there is no significant change of relative intensity of spectral components.

$\Delta E_{k+1} = F^*(x_{k+1}) \cos(2\pi \nu_j x_{k+1}) \Delta x$  is calculated by summing small increments, i.e.

$$\begin{aligned} \Delta E_{k+1} &= \sum_{\nu} d_{\nu} [F^*(x_{k+1}) \cos(2\pi \nu x_{k+1})] \Delta x \\ &= \sum_{\nu} F^*(x_{k+1}) d_{\nu} [\cos(2\pi \nu x_{k+1})] \Delta x, \end{aligned} \quad (5)$$

where  $d_{\nu}$  is used to indicate that the increment is for a constant value of

$x_{kH}$ ,  $\nu$  being the variable for the moment.

At every moment that the increment  $d_\nu[\cos(2\pi\nu x_{kH})]$  reaches +1 unit or -1 unit, the gate (I) is operated and  $F(x_{kH})$  is added to or subtracted from the previous value of  $\Delta E_{kH}(\nu_j)$ , which is the content of the first accumulator, until  $\sum d_\nu[\cos(2\pi\nu x_{kH})]$  reaches  $\cos(2\pi\nu_j x_{kH})$  for given  $\nu_j$  and  $x_{kH}$ . The content of the accumulator is transferred to the second accumulator by operating the gate (II) by the signal pulse which indicates  $\nu = \nu_j$ .

The increment  $d_\nu[\cos(2\pi\nu x_{kH})]$  is generated by using two integrators and three coefficient-multipliers as in a digital differential analyzer.<sup>4)</sup>

The computer is of the incremental type. Therefore it is simple as compared to the general-purpose digital computer which is of integral type. The results of the calculation, i.e. intensities of the spectral components, are displayed on a monitoring c.r.t. screen at any instant by reading the stored values of  $E_k(\nu_j)$ 's out of the memory and converting digital values to analog by the D-A converter. The horizontal axis is synchronized to the period of  $\Delta x$  and  $E_k(\nu_j)$ 's are given as vertical deflections. More precise values can be plotted on an X-Y recorder at the end or at any moment of scanning of the interferometer, if desired.

#### References

- 1) H.A.Gebbie: I.C.O.5th Conf. Stockholm (1959).
- 2) G.R.Harrison, N.Sturgis, S.C.Baker and G.W.Stroke: J.O.S.A. 47,15(1957).
- 3) J.Guild:"The Use of Diffraction Gratings as Scales", Oxford University Press, New York, 1960.
- 4) R.E.Sprague: MTAC, 6,41 (1952)



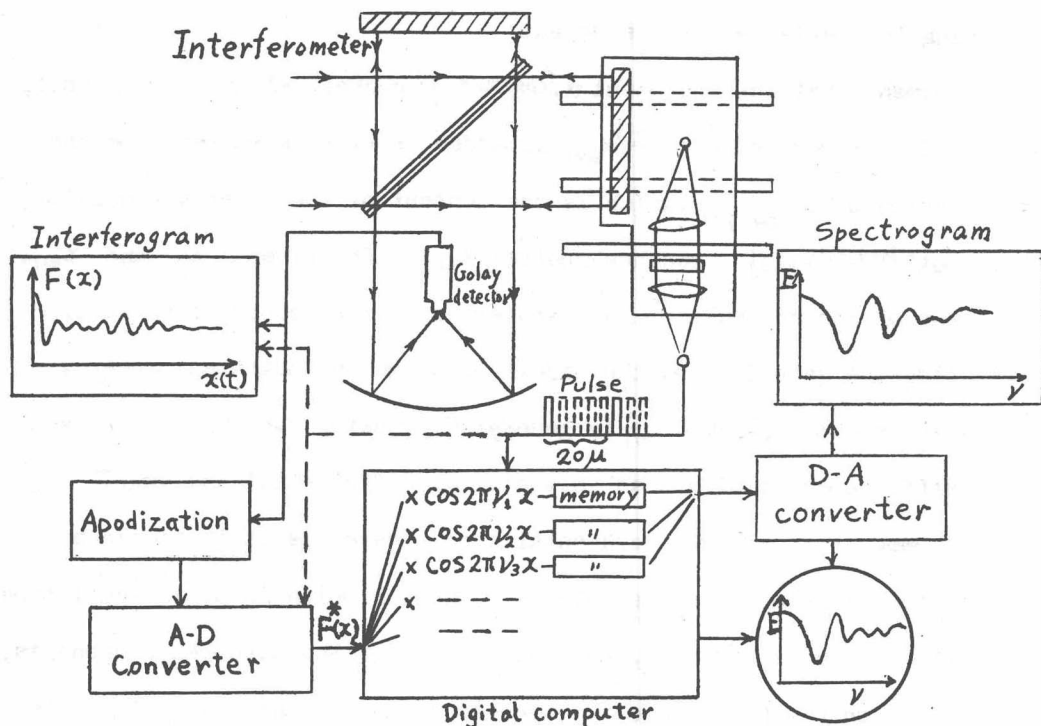


Fig. 1. Block diagram of the far infrared automatic-recording interferometric spectrometer.

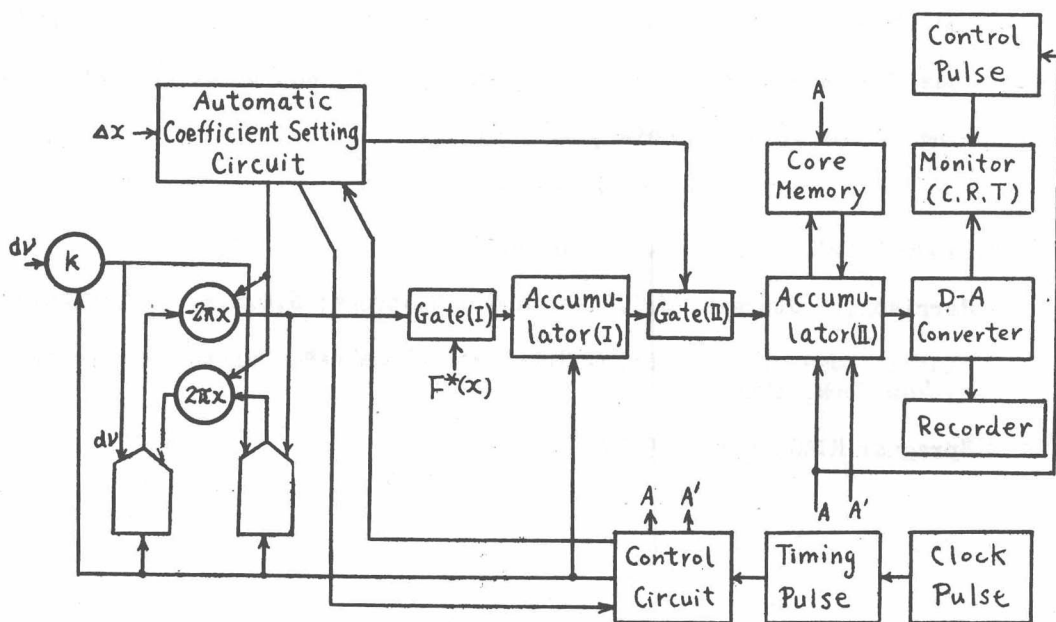


Fig. 2. Block diagram of the digital computing unit



# An Interferometric-Modulation Order-Separator for a Far Infrared Spectrometer\*

Miles E. Vance, Robert F. Rowntree, Ely E. Bell and Robert A. Oetjen

Laboratory of Molecular Spectroscopy and Infrared Studies, Department of Physics and Astronomy, The Ohio State University, Columbus, Ohio

Gebbie (1) and Strong (2) have used two-beam interferometers to obtain far infrared spectra by Fourier transformation. Genzel and Weber(3), (4) have worked their interferometric modulator periodically to obtain a spectrum directly through the use of narrow bandpass electrical filtering of the modulated detector output. Following the suggestion of Strong(5) and of Genzel (3) we have constructed a periodically-operating lamellar-grating interferometric modulator for use as an order-separator for a conventional grating spectrograph in the wavelength region 100 - 1000 $\mu$ .

In the ideal operation of the modulator the movable part of the lamellar grating reciprocates with constant speed so that the path difference  $x(t)$  varies as shown in Fig. 1 (a). The maximum path difference  $x_m$  is set so that for a certain wave number  $\nu_n = \frac{1}{\lambda_n}$  the lamellar grating output power, or the modulation function, passes through a selected integral number  $n$  of modulation cycles while the path difference varies by the total amount  $2x_m$  during the period  $T$ . That is, radiation of wave number  $\nu_n$  is modulated sinusoidally at frequency  $f_n = \frac{n}{T}$  if the maximum path difference is set so that  $2x_m = n\lambda_n$ . The detection system is tuned to the fixed frequency  $f_n$  by means of synchronous rectification at frequency  $f_n$  and appropriate electrical filtering.

Scanning is done by varying the amplitude of the reciprocating motion. This changes the value of the wave number  $\nu_n$  modulated at the

\*Supported in part through a grant from the National Science Foundation and a contract between The Ohio State University Research Foundation and Air Force Cambridge Research Laboratories.

fixed frequency  $f_n$ . The spectrometer grating drive and the modulator scanning drive are mechanically coupled so that the wave number of the radiation in the first order of the spectrometer is the same as  $\nu_n$  of the modulator. With this arrangement, the spectral response of the combination, i.e., the contribution of incident wave number  $\nu$  to the output signal for a given value of the scanning variable  $\nu_n$ , is the product of the spectral response of the modulator and that of the spectrometer.

The ideal modulator spectral response is

$$S_o(\nu, \nu_n) = \text{dif } \frac{n}{\nu_n}(\nu - \nu_n) + \text{dif } \frac{n}{\nu_n}(\nu + \nu_n)$$

where  $\text{dif } y = \frac{\sin \pi y}{\pi y}$ . This is shown in Fig. 1 (c) for  $n = 3$ . The half-width of the main peak at  $\nu_n$ , as well as the spacing of the zeros of the curve, is  $\frac{\nu_n}{n}$ . The resolving power of the modulator alone may thus be defined as  $\nu_n \div \frac{\nu_n}{n} = n$ . The dotted triangles in Fig. 1 (c) represent the spectrometer spectral response  $S_m(\nu, \nu_n)$ . In normal operation we use  $n = 13$ , but the spectrometer spectral slit width is always kept narrower than the main peak of the modulator spectral response. The overall resolution is that of the spectrometer. For an input spectral distribution  $P_o(\nu)$  the output signal for a given value of  $\nu_n$  is

$$\int_{-\infty}^{\infty} P_o(\nu) S_o(\nu, \nu_n) S_m(\nu, \nu_n) d\nu$$

Since  $S_o(\nu, \nu_n)$  passes through zero at  $2\nu_n, 3\nu_n$ , etc., the contributions of the higher spectrometer orders are very small.

Perhaps the most crucial adjustment of the modulator is in the location, relative to the fixed part of the grating, of the center about which the movable part of the grating oscillates. In the two-sided operation of the modulator illustrated by Fig. 1 (a) this center must be exactly at the position of zero path difference, or "mirror position". A small displacement of this center corresponding to a path difference error  $x_0$  reduces the peak of  $S_o(\nu, \nu_n)$  by the factor  $\cos 2\pi \frac{x_0}{n}$ .

Description. -- A plan drawing of the complete spectrographic system is found in Fig. 2. It consists of source-, sample-, monochromator-, modulator-, and detector-units. Each unit is contained in a separate vacuum tank to allow rearrangement of units. The source is a 250 watt mercury lamp. The sample unit optics can be arranged for reflection or transmission measurements of cooled samples. The reststrahlen holders and conventional chopper in the source and sample units are used only for wavelengths less than about  $100\mu$ , when the modulator is not being used. The monochromator has a f/4 Czerny-Turner mounting, as does the modulator. The dispersion gratings are blazed at 100, 200, 400, and  $800\mu$ . Black polyethylene and the crystal quartz window of the Golay detector serve as transmission filters. The entire instrument is evacuable.

Results. -- The modulator has shown good filtering properties throughout the region 100 -  $1000\mu$ . Some water vapor spectra obtained with the instrument are shown in Figs. 3 and 4. Strong absorption lines yield zero signal and higher order absorption lines are absent. The calculated line positions and intensities were obtained from Benedict.\* Fig. 4 gives an idea of the resolution so far attained. Quantitative tests at several wavelengths indicate a spectral purity of a least 96% away from blaze and 90% at blaze.

#### References

1. H. Gebbie, N. Stone, and C. Walshaw, *Nature* 187, 765 (1960).
2. J. Strong, *J. Opt. Soc. Am.* 47, 354 (1957).
3. L. Genzel and R. Weber, *Z. angew. Physik* 10, 127 (1957).
4. L. Genzel and R. Weber, *Z. angew. Physik* 10, 195 (1957).
5. J. Strong, *J. Opt. Soc. Am.* 44, 352 (1954).

\*Private communication

Fig. 1. (a) The ideal path difference variation (b) The modulation function for arbitrary  $\nu$  (c) The spectral response for  $n=3$

$$x(t) = \frac{2x_m}{T} t \quad \left(-\frac{T}{2} < t < \frac{T}{2}\right)$$

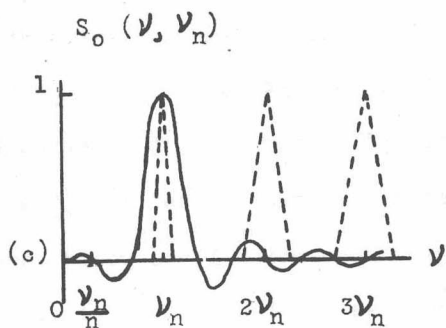
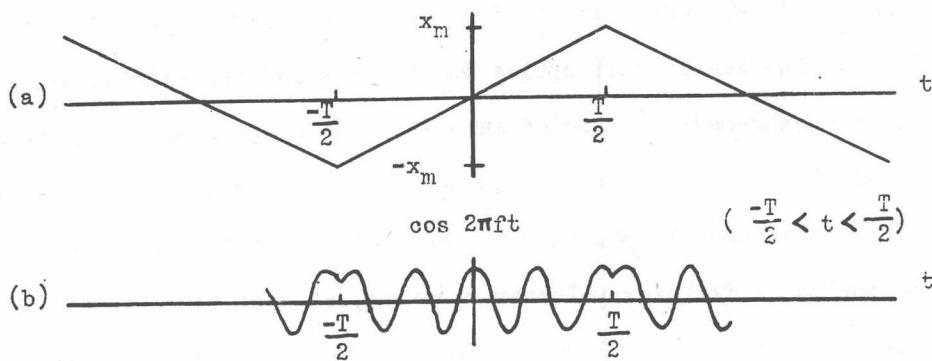


Fig. 2

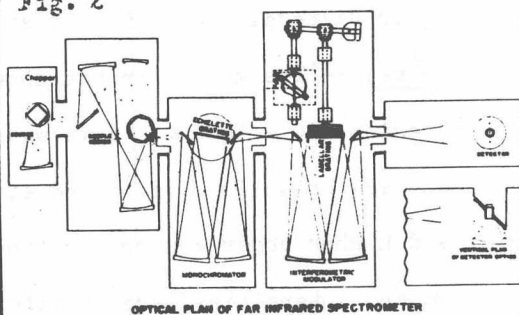


Fig. 3

WATER VAPOR ABSORPTION AT ATMOSPHERIC PRESSURE  
0.31  $\text{cm}^{-1}$  SPECTRAL SLIT WIDTH 5.5 mm SLITS

CALCULATED LINE POSITIONS & INTENSITIES:

41.00	42.62	44.12	47.05	48.02	51.44	53.48
1625.	23.02	187.4	4837.	30.30	49.76	2320.

GRATING BLAZE

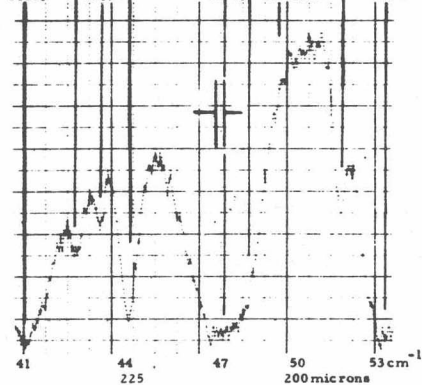


Fig. 4

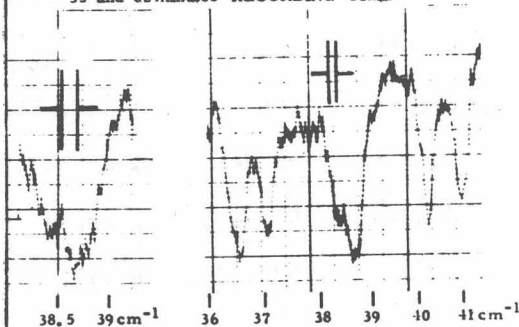
WATER VAPOR ABSORPTION

20 mm Hg PRESSURE

0.16  $\text{cm}^{-1}$  SPECTRAL SLIT WIDTH

45 sec TIME CONSTANT 4.5 mm SLITS

35 and 82 minutes RECORDING TIME



## An Optical Null Double Beam Far Infrared Spectrometer

Hiroshi Yoshinaga, Shegeo Minami and Akiyoshi Mitsuishi  
(Department of Applied Physics, Osaka Univ., Osaka, Japan)

Isao Makino, Koroku Nakamura, Isao Iwahashi, Masao Inaba  
and Koichi Matsumoto  
(Naka Works, Hitachi Ltd., Ibaraki, Japan)

### 1, Introduction

In making measurements in far infrared region from  $500\text{ cm}^{-1}$  to about  $60\text{ cm}^{-1}$ , a compact far infrared spectrometer which is adaptable both to single-beam and double-beam operations using optical null principle is constructed for laboratory and industrial uses. The design of the instrument was especially carried out with the view of compact construction and easy operation at room temperature measurements.

As extremely small radiant energy is available in far infrared spectrometers, it is understandable it would be very difficult to make a far infrared spectrometer which has high qualities in any features. Most measurements of molecular spectra of gases used to be made at room temperature. According to the mathematical analysis, the optical null method is one of the best way in the various kinds of double-beam photometric systems as far as the signal to noise ratio is concerned. Taking into consideration the efficient use of energy, the authors adopted the optical null method to the far infrared spectrophotometer in spite of its shortcomings in low or high temperature measurements. Provision is made in this instrument for either double-beam or single-beam operation with turning knobs. The single-beam operation is used in the measurements of the samples kept below or above room temperature.

### 2, Optical System

Fig. 1 shows a schematic layout of the optical system. Two radiation

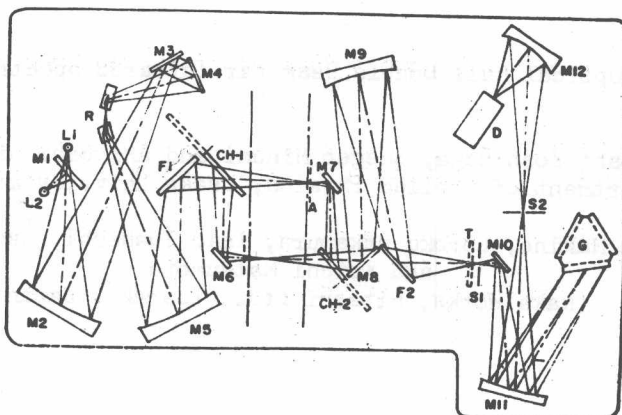


Fig. 1

sources, that is, a global L1 for the measurements down to  $125\text{ cm}^{-1}$  and a high pressure mercury lamp L2 below  $125\text{ cm}^{-1}$ , are used and either one can be switched into correct location in the optical pass by sliding a plain mirror M1. Reststrahlen filtering system is composed of two filter wheels in which six kinds of Reststrahlen crystals are held in each one, so as to keep the reflection surfaces of the two crystals crossed. CH-1 and CH-2 are a beam splitting and a beam combining sector mirrors for double-beam system, which are rotated at 10 rps. T is a filter wheel of transmission filters, which can hold 6 filters.

Conventional Littrow type arrangement is used for monochromator optics. The height of the slits is 12 mm and the maximum opening is 10 mm. A 20 degree off-axis parabolic mirror of about 290 mm focal length is used as a collimator mirror M11. Three plane gratings of which ruled area is 64 mm x 64 mm are mounted on a trigonal-prism shape holder G. The first order spectrum of each grating is used to cover the whole wavenumber region from 500 to about  $60\text{ cm}^{-1}$ . The dispersed beam from the exit slit is converged with 60 degree off-axis ellipsoidal mirror M12 on Golay cell after getting 5 x image reduction.

Two scatter plates with roughened surface are mounted at F1 and F2.

### 3, Mechanical Construction

The whole optical components and a part of driving mechanisms are

mounted on the base of a vacuum tank usually kept at about 0.01 mm Hg during the operation. Besides the grating positioning motor, all motors are mounted outside the tank and mechanically connected to the mechanisms located in the tank with O-ring seal through the base. Amplifiers, control electronics and power packs for radiation sources are located under the tank and controlled with switches on the panel from the front side of the instrument. A recording part is placed in front of the tank and easily observed from the operator's position. Pilot lamps and a wavenumber dial beside the recorder indicate the successive process of the operations.

#### 4, Control and Recording System

The output signal from the Golay cell, after amplification at 10 cps. is fed into a phase sensitive rectifier which is operated with the reference signal from the generator connected to the beam switch. A conventional servo-system is used to control the comb-shaped beam attenuator for the double-beam operation. To permit the single-beam operation the single amplifier system has linearity, and rectified signal is directly recorded with the recorder by using a electronic feed back system.

The slit drive is given either manually or automatically with a slit driving servo-system.

Full automatic operation is provided by pushing the start button. All operations including grating change and filter insertion are scheduled with microswitches operated with the actuator located on the wavenumber cam shaft. To make accurate recording at the borders between one grating and the other in scanning operation, the scanning drive is so controlled that the transmission curves with both gratings are overlapped at their changing positions.

The mechanical clutches in the scanning gear trains permit selection of scanning speed in six steps from 3.2 to 0.1 cm / min. by turning a knob



TABLE I

Spectral range ( $\text{cm}^{-1}$ )	Grating ( $\text{L/mm}$ )	Reststrahlen filter	Transmission filter	Scatter plate
500 - 400	30	LiF		Two 800 mesh roughened plate
400 - 260	"	NaF		"
260 - 180	"	BaF <sub>2</sub>	BeO ZnO Powder filter	"
180 - 142	20	KCl		"
142 - 125	"	KBr		"
125 - 60	8	TlCl	Sooted quartz plate BeO ZnO NaF KCl Powder filter	"

on the front panel. Extremely slow scanning speed ranges are also available with manual change of the gears. The schedules of the automatic scanning wavelength range is readily provided by using a scanning programmer on the panel, which is operated with scanning gear shaft.

### 5, Operations and Performance

The desirable results have been obtained in the wavenumber region from  $500 \text{ cm}^{-1}$  to  $60 \text{ cm}^{-1}$  both in the single-beam and the double-beam operations. The combinations of the Reststrahlen crystals, scatter plates and transmission filters in each spectral range are shown in Table I. Spectral purity was satisfactory and the experimental results showing this filtering effect will be presented with slides.

The absorption curves of water vapor will also be shown in detail with slides. These curves show <sup>that</sup> the average resolution in almost all wavelength region, except near the longest wavelength side, is about  $0.5 \text{ cm}^{-1}$  both in the single-beam and the double-beam operations.

This report is on a prototype instrument and the commercial ones will be manufactured after a number of improvements on this prototype model.

## Far Infrared Experimental Techniques

Ludwig Genzel

Physikalisches Institut der Universität Freiburg  
Freiburg i. Breisgau, Germany.

The intention of this paper will be to give a survey over some experimental methods for far infrared spectroscopy. In many aspects the instrumentation differs here quite markedly from that of other spectral regions, though it combines the typical aspects of the neighbouring microwave and near infrared techniques. Besides the main conventional methods special emphasis is directed to recent developments and future possibilities. The paper will be limited to the more important questions concerning radiation sources, detectors and spectrometry.

A. Sources of Radiation.

The classical sources are the high pressure mercury arc ( $\sim 1$  atm.) for the 100 to 10 wavenumber range and the gas heated Welsbach mantle for the 250 to 100 wavenumbers range. The latter source can be modified for electrical heating by putting the Welsbach mantle onto a small hollow cylinder of a good reflecting and temperature stable metal like some platinum alloys to assure low emissivity in the near infrared.

The Hg-arc emission is limited on the high frequency side due to the increasing absorption of the quartz envelope and the decreasing absorption and emission of the plasma. After having its highest emission around  $40\text{ cm}^{-1}$  - a black-body radiation of  $5000^\circ\text{K}$  - there is a rapid decrease to lower wave numbers ( $\nu^4$  to  $\nu^8$ ) due to the increasing selfabsorption of the colder plasma zones toward the envelope (1). Despite this some authors were able to detect this radiation up to  $5\text{ cm}^{-1}$  and lower (2). But the limitation for using the mercury arc as a spectroscopic source is around 20 to 12 wavenumbers.

Some newer developments can be expected from sources which use the emission of accelerated electrons. Several types are already investigated in the neighbouring regions: The undulator (3), the Smith-Purcell source (4) and the Cerenkov source (5), which are very similar in their emission characteristics and where the Cerenkov source is under comparable circumstances generally the best one. The efficiency of these sources is first strongly dependent from